Journal of Scientific & Industrial Research
Vol. 84, December 2025, pp. 1310-1321
DOI: 10.56042/jsir.v84i12.15335

Adam Red Panda Optimization for Detection and Severity Level Classification for Lung Cancer using CT Image

Alok Kumar[1]*, Ankur Prakash[4], Ajeet Kumar Srivastava[2], Vishal Awasthi[2], Pushpa Mamoria[3], Deepak Kumar Verma[1], Amit Seth[5], Vineeta Singh[1*], Kapil Joshi[6] & Vandana Dixit Kaushik[7]

[1]Department of Computer Science and Engineering, [2]Department of Electronics and Communication Engineering, [3]Department of Computer Applications, School of Engineering and Technology (Formerly known as UIET Kanpur), Chhatrapati Shahu ji Maharaj University, Kalyanpur, Kanpur, Uttar Pradesh 208 024 U.P. India

[4]Department of Computer Science and Engineering, MNNIT Allahabad

[5]Department of Computer Science and Engineering, Sharda School of Computer Science and Engineering, Sharda University, Greater Noida

[6]Department of Computer Science & Engineering, Uttaranchal Institute of Technology (UIT), Uttaranchal University Dehraudn 248 007, Uttarakhand, India

[7]Department of Computer Science and Engineering, Harcourt Butler Technical University, Nawabganj Kanpur, HBTU East Campus 208 002, Kanpur, India

Received 27 November 2024; revised 13 June 2025; accepted 18 December 2025

Lung cancer is the leading cause of death worldwide, estimated to give rise to almost 7.6 million deaths annually. Early diagnosis is crucial in order to minimize fatalities associated with lung cancer. Two major imaging tests are Computed Tomography (CT) scans and chest X-rays, which are useful in diagnosing lung cancer. One of the major causes of death in the world today is lung cancer, and early detection and treatment is the key to successful management. Traditional methods of diagnosis, such as CT scans, have problems of accuracy and efficiency. This paper introduces a novel deep learning model, ARPO NasNet, which applies Adam Red Panda Optimization (ARPO), a novel optimization technique developed by the authors, to achieve better performance in detecting and classifying the severity of lung cancer based on CT scans. RPO (Red Panda Optimization) is a recently developed metaheuristic algorithm inspired by the behavioral characteristics of red pandas, which enhances the optimization process. The proposed method involves preprocessing CT images with median filters to remove noise, Deep Fuzzy Clustering (DFC) for segmentation of lung lobes, and Local Gradient Patterns (LGP) for feature extraction. The ARPO algorithm optimizes the NasNet model, improving its classification accuracy, precision, recall, and F1-score, thereby outperforming state-of-the-art methods. The proposed methodology demonstrates significant breakthroughs in lung cancer detection and the grouping of its severity phases, offering a solution for early and accurate diagnosis of lung cancer. Such results suggest the potential of ARPO_NasNet in clinical applications for the detection and treatment of lung cancer.

Keywords: Classification, Deep fuzzy clustering, Disease prediction lung cancer detection, Neuron attention stage-by-stage network, Optimization

Introduction

Lung cancer occurs in both men and women and is a major cause of death worldwide.[1] The need to diagnose early is paramount in enhancing survival, yet it proves to be a great challenge because many of the symptoms manifest themselves at an advanced stage.[2] Patients that are above 50 years are especially vulnerable.[3] The disease may be hard to detect on time due to complications with the progression of the disease.[4] The mortality rate of lung cancer is the highest among all cancers worldwide.[5] Early detection of lung cancer significantly improves survival rates. According to the American Cancer Society, the five-year survival rate for patients diagnosed at an early stage is around 56%, compared to just 5% for those diagnosed at advanced stages. This highlights the critical need for early diagnosis to increase survival and reduce treatment costs. CT scans are essential tools for diagnosing lung cancer by detecting nodules, but interpreting these scans requires expert knowledge. Besides, radiologists are overworked to scan and examine many scans, which drives the necessity of automation.[6]

The Computer-Aided Diagnostic (CAD) developments have also provided alternatives of

*Authors for Correspondence
E-mails: vineeta.singh.cs@gmail.com, alok@cjsmu.ac.in

automatically identifying lung cancer based on CT scans and this has greatly helped radiologists.[7] Conventional approaches, though, tend to be restricted by ineffectiveness in working with extensive datasets and multifaceted image attributes.[8] Deep learning (DL) methods have become potent in terms of improving the analysis of medical images.[9] DL is also excellent at learning to detect features automatically in images and thereby enhancing accuracy of detection.[10] Techniques such as segmentation are important in that they divide images into small manageable parts that may produce features of interest.[11] These advances notwithstanding, reliability is still a problem, with most of the approaches, yet, having difficulties with optimization in practice.[12]

This paper is aimed at addressing these drawbacks by introducing a new hybrid approach known as ARPO NasNet to detect lung cancer.[13] The approach is a composite of Adam Optimization and Red Panda Optimization (RPO): is a novel optimization technique proposed by the authors it solves the typical optimization issues encountered with classical models. Adam can be used to adjust the learning rates and RP is used to boost the global search ability which results in more robust and quicker convergence in the process of training.[14] Earlier research tended to employ Adam singly and this may be sluggish when using sophisticated imaging data.[15] ARPO_NasNet takes advantage of these two optimizers to enhance the performance of the models particularly in the convergence speed and classification accuracy.[16]

The ARPO_NasNet model operates in a few steps: Preprocessing of images with the help of a median filter to eliminate noises, the lung lobes segmentation with Deep Fuzzy Clustering (DFC), and extraction of features with the help of Local Gradient Pattern (LGP).[17] Lastly, NasNet would classify lung cancer when optimized by ARPO. This process classifies the results as normal or abnormal and the severity into mild, moderate or severe.[18] The results of ARPO NasNet are demonstrated to be higher than the conventional procedures, its accuracy, reliability, and efficiency are better and provide a more robust solution to lung cancer detection that may be applied in the practice environment.[19]

Even though the methods of deep learning have advanced lung cancer detection, most of the current methods use traditional optimization techniques such as Adam that may be slow and fail to work with complex medical images, and is sometimes not applicable when dealing with large datasets or high levels of classification. In this paper, a new method, the ARPO, is presented as a combination of Adam and Red Panda Optimization (RPO). The hybrid approach is based on the learning rate adaptations of Adam and the global search resulting in RP, where optimizing becomes more efficient. The combination of these two approaches allows the ARPO_NasNet model to be more accurate, more precise, more recalls, and more F1-score than the current models, but it also offers more reliable and effective solution to lung cancer detection.

Literature Survey

A summary of the literature showing the progress in the intended field of study is presented in Table 1. NasNet is a deep learning architecture that has been applied to detect lung cancer in many studies, with an aim of increasing the accuracy of the method by improving the processing of the images. Nevertheless, these models mostly use one optimization strategy, e.g., Adam, which performs well yet might be not capable of coping with the complexity of medical images. A hybrid between Adam and Red Panda Optimization (RPO)[33] is required to advance the way the model learns. The model is also useful since it allows the Adam to explore more optimal solutions with the aid of RPO. This mixture amplifies efficiency, which improves the model in identifying lung cancer. Our ARPO NasNet model is faster to learn, processes larger datasets more efficiently and yields superior quality results, thereby offering a more robust and dependable solution to deep learning in medical image analysis.

There has been significant advancement in medical image analysis involving deep learning and optimization techniques significantly improving diagnostic performance. Multichannel feature-fusion networks[35], adaptive masked autoencoders[36], and Convolution–Transformer hybrid models[37] have shown strong capability in extracting meaningful features out of complex biomedical images. Enhanced transformer-based segmentation techniques such as CenterFormer[38] and graph deep learning techniques for vascular assessment[39] further shows the significance of advanced representation learning in clinical applications. Weakly supervised transformer models have also achieved promising results in tumor diagnosis and biomarker identification[40], while optimization-driven segmentation strategies, including ant-colony–based MRI analysis[41], emphasize the

Table 1 — Literature review

Aim[Ref]	Method	Advantages	Disadvantages
Detect lung tumors using deep learning models (RNN-GAN)[20]	RNN + GAN for automated lung tumor detection	Increased accuracy and efficiency in lung cancer detection	Did not optimize for accuracy in practical applications
Detect lung cancer with fewer computational resources[21]	DenseNet-121 + MobileNet V3	Low-cost, resource-efficient model	Performance issues with maintaining robustness
Lung cancer classification using optimization techniques[22]	PSSO-based deep residual network (DRN)	Faster detection and classification	Optimization method not effective in improving accuracy
Detect and classify severity of lung diseases[23]	CNN (MixNet) with dense block (MixNet-LD)	Improved performance and generalizability	Failed to classify severity levels accurately and quickly
Enhance lung cancer classification accuracy[24]	EOSA-CNN (Ebola Optimization search algorithm + CNN)	Superior accuracy, reduced false positives	Limited sample size, unbalanced data, time complications
Develop a real-time lung cancer detection system[25]	DenseNet-121, CNN with MobileNet V3 for feature extraction	Real-time detection, aids in early diagnosis	Lacked liquid neural networks or ensemble learning methods
Assess the effectiveness of AI frameworks in lung cancer detection[26]	Systematic review and meta-analysis of AI frameworks	High diagnostic accuracy using AI	Reported diversity in AI models' performance
Identify lung cancer using DenseNet and attention mechanism[27]	DenseNet with ATT-DenseNet attention mechanism	Improved lung cancer identification	Optimization issues, not applicable for real-time use
Evaluate DL for lung cancer screening and diagnosis[28]	Deep learning for classification and segmentation	Promising accuracy for lung cancer screening with CT images	Limited to classification and segmentation
Automate malignant cell detection in lung tissue images[29]	Image prediction with explainability	Explanation of regions relevant to lung cancer	Lacked integration with clinical workflows
Detect lung cancer at early stages to improve survival rates[30]	LSTMs (Long Short-Term Memory networks) + VGG-19 CNN	Early detection of lung cancer	Focused more on image segmentation, not on classification
Classify lung cancer as benign, normal, or malignant[31]	Exceptionally Randomized Tree Classifier + VGG16	Multi-class lung cancer classification	Limited by the classifier's accuracy in complex cases
Use deep learning for faster lung cancer diagnosis[32]	Deep learning algorithms with a focus on optimization	Reduces diagnosis time and increases accuracy	Relies on large, well-labeled datasets, can struggle with imbalanced data

value of metaheuristic methods in improving prediction accuracy. Building on these developments, the present work proposes an Adam Red Panda Optimization–based framework for the detection and severity classification of lung cancer using CT images, aiming to support precise and reliable clinical decision-making.

Research Gap

Despite many deep learning architectures proposed to detect lung cancer like CNN, DenseNet, GAN and optimization-based methods, they are still facing major drawbacks that are: inefficiency in optimization, decreased performance on complicated and imbalanced data, limited performance in classification at various levels of severity, poor generalization of diverse CT scan images and lack of real-time usability in emergency departments. In response to all these gaps, the proposed ARPO_NasNet model combines Red Panda Optimization (RPO) with Adam optimization to improve convergence and global search capacity, boosts detection ability on complex and imbalance data, guarantees better accuracy and reliability, and facilitates scalable and real-time deployment in order to achieve effective lung cancer screening.

Proposed ARPO_NasNet for the Lung Cancer Identification and Severity Level Classification

This article introduces a hybrid technique, ARPO_NasNet for the identification and lung cancer severity level classification. At first, the CT image is pre-processed by employing a median filter to eliminate to noise present in the input CT image. Red Panda Optimization (RPO) is a novel optimization technique, inspired by the foraging and climbing behaviours of red pandas. RPO was designed to enhance the optimization process by improving global

search capabilities and accelerating convergence during training. Afterward, the lung lobe segmentation is performed by applying DFC, and then, feature extraction is done with the help of LGP. Later, lung cancer classification has been done with NasNet, which is tuned by ARPO. Here, the ARPO is designed by the integration of Adam Optimization and RPO. The detected outcome is categorized as abnormal and normal. Further, in the case of abnormal output being detected, the disease severity level is categorized as severe, moderate, and mild by applying NasNet with ARPO. The pictorial demonstration of the presented ARPO_NasNet model is depicted in Fig. 1

Dataset

Image collection in the Lung Image Database Consortium image collection (LIDC-IDRI) is an internationally distributed publicly available open dataset of thoracic CT scans developed with the collaboration of seven academic centres and eight medical imaging corporations and funded by the NCI, further developed by the FNIH and facilitated by the FDA. It includes 1,018 cases of CT images and a corresponding XML file of lesion annotations during a two-step review procedure by four thoracic radiologists, first during an independent blinded review phase of case annotations, followed by an unblinded phase during which radiologists revised lesion annotations by reviewing anonymized peer marks. The aim of the dataset is to fully represent the lung nodules without forced consensus, which is an essential resource to develop, train, and evaluate

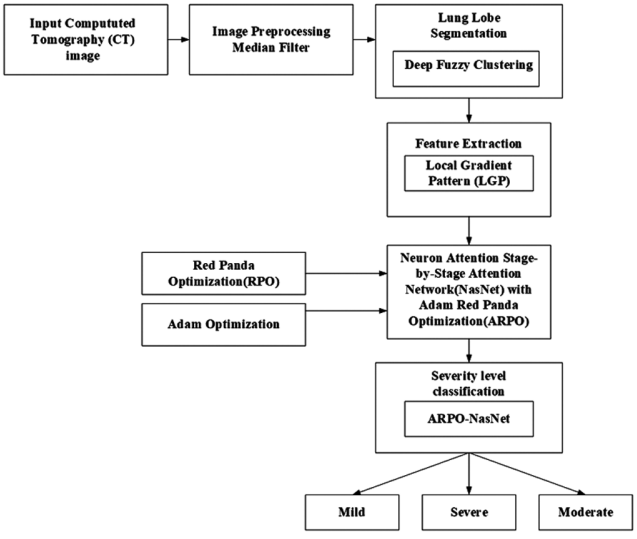

Fig. 1 — Proposed ARPO_NasNet Model

Computer-Aided-Diagnostic (CAD) systems in lung cancer detection and diagnosis. It is suggested to the users to first concur with such tools as pylidc and standardised DICOM-LIDC-IDRI representations before constructing custom analysis pipelines using the XML data.[34]

Image Acquisition

The dataset of CT images is first collected to serve as the basis for lung cancer detection and severity classification. Each image in the dataset represents a candidate case, and preparing this dataset correctly is critical for building a reliable model. The Computed Tomography image is assimilated from the dataset Y is contemplated to attain detection as well as the classification of the severity levels of lung cancer and the dataset is designated as

$$\mathcal{D} = \{X_1, X_2, \dots, X_n\} \quad \dots (1)$$

where, $\mathcal{D}$ denotes the represents the dataset, which is a collection of CT images, $X_1, X_2, \dots, X_n$ denotes the individual images in the dataset. This is the standard way to represent a set of elements (in this case, images) in mathematics.

Image Pre-processing

CT scans often contain noise, which can negatively impact segmentation accuracy. To address this, a median filter is applied, as it effectively reduces salt-and-pepper noise while preserving edges and important lung details. The pre-processing process is performed by applying a median filter for removing the noise that is present in the input image Y_p. The median filter is demarcated as the nonlinear image processing method concerning statistics theory on categorization that effectively eliminates noise. Besides, this filter secures the information present at the image edge. The expression of the median filter is given by,

$$\hat{Y}_p = median\{Y_q \mid q \in \mathcal{N}(p)\} \quad \dots (2)$$

where, N(p) is the neighbourhood of pixel p. The resulting denoised image is then forwarded to the segmentation stage for isolating lung lobe.

Lung Lobe Segmentation

After denoising, the next step is to isolate lung lobes from the CT image. This is achieved using Deep Fuzzy Clustering (DFC), which combines deep learning's representation power with fuzzy clustering

for precise segmentation. The preprocessed image A_i is forwarded to the lung lobe segmentation block. Here, DFC is employed for isolating the lung lobe. The DFC performs effectual clustering, using the Deep Neural Network (DNN's) ability of representation learning and the concept of fuzzy clustering. In DFC, the two matrices: a fuzzy within-cluster scatter matrix T_1, and fuzzy between-cluster scatter matrix T_2 are used, and they are designated as,

$$S_w = \sum_{i=1}^{N} \mu_i (x_i - c_i)(x_i - c_i)^T \quad \ldots (3)$$

$$S_b = \sum_{i=1}^{N} \mu_i (c_i - \bar{c})(c_i - \bar{c})^T \quad \ldots (4)$$

where, d denotes the dimensionality of the input image, referring to the number of pixels or features in the image, μ_i denotes the membership degree of the i-th image feature or pixel to a particular cluster, c_i denotes the center of the cluster, which represents the centroid of the i-th cluster, γ denotes the fuzzifier, a parameter that controls the level of fuzziness in the clustering process, N denotes the total number of clusters considered in the clustering process, X_i denotes the training image input, where X_i is the pixel or feature value being considered for clustering, $\bar{c}$ denotes the average of the overall image, which is often used to represent the mean value of pixel intensities or features in the image.

Here, A_i represents the individual CT image features (pixel intensities) used as inputs to the clustering process. From these features, the fuzzy scatter matrices $h(r,t)$ are computed, where $h(r)$ measures the within-cluster scatter and $h(t)$ measures the between-cluster scatter. Thus, A_i serves as the raw input, while $h(r,t)$ represents the statistical functions derived from A_i during Deep Fuzzy Clustering.

For reducing the distance within a class as well as to increase the distance from the information to the mean the loss function given below is applied, which is expressed as

$$L = \sum_{i=1}^{n} \left(\|x_i - \mu_c\|^2 + \lambda \cdot \|\mu_c - \mu\|^2 \right) \quad \ldots (5)$$

where, x_i represents a feature from class $c_r \mu_c$ is the mean of class c_r and μ is the overall mean. The term λ is a hyperparameter controlling the trade-off between the within-class and between-class distance.

$$\frac{\partial L}{\partial \theta} = \sum_{i=1}^{n} \frac{\partial (\|x_i - \mu_c\|^2)}{\partial \theta} \quad \ldots (6)$$

where, θ represents the model parameters. The fuzzy membership operation e_{ql} is termed as

$$\mu_i(x) = \frac{1}{1 + \left(\frac{\|x - \mu_i\|}{\delta} \right)^2} \quad \ldots (7)$$

where, μ_i is the center of the i-th cluster, and δ is a parameter controlling the spread of the membership function.

Hence, the segmented lung lobe I_e is attained by applying the pre-processed outcome to the DFC and this is then subjected to feature extraction. The segmented lung lobes ensure that subsequent feature extraction is performed only on the most relevant regions of the CT scan

Feature Extraction

The lung lobe segmentation outcome I_e is given to the process of mining of features, where LGP is mined. The LGP[18] is utilized for several image classification applications. For specific pixels J_f, firstly LGP attains the neighbourhood $J \times J$ and records the value of the gradient, s_c of an adjacent pixel J_f as$s_c = \left| J_c - j_f \right|$ for producing the disparity of local intensity. Then, the average of the gradient value for G adjacent pixels, s_y is calculated by employing arithmetic mean as $s_y = \frac{1}{G} \sum_{c=0}^{G} s_c$ which is applied as the threshold. Later, the gradient value of every neighboring pixel is compared with a threshold to identify whether the binary value is 0 or 1. At last, the binary number sequence random path is coded as the equal decimal value and allocated to the pixel at the center. Once the lung lobes are segmented, the next step is to extract discriminative features. We employ Local Gradient Pattern (LGP), which captures local intensity variations in CT images and encodes them into robust numerical descriptors

$$l\,g\,p_{G,j}\left(u_f, v_f\right) = \sum_{c=0}^{G-1} r_1 \left(s_c - s_y\right) 2^c \quad \ldots (8)$$

$$r_1(f) = \begin{cases} 1 \; iff \geq 0 \\ 0 \; otherwise \end{cases} \quad \ldots (9)$$

where, f signifies the variance among the threshold, and s_y its adjacent gradient, the coordinate of the center pixel is signified as $\left(u_f, v_f\right)$, and the radius is termed as j. The outcome attained from the feature extraction module is implied as H. The extracted feature vectors are then used as inputs for classification by the NasNet model.

Lung Cancer Detection

The feature excerpted H is further applied to the lung cancer detection module. Here, NasNet is

employed to detect lung cancer. NasNet[31] is a family of DL techniques. The structure of the NasNet is flexible and thus it can adapt to various tasks comprising object detection, semantic segmentation, and image classification. Here, the NasNet is trained using the ARPO algorithm, which is generated by combining the Adam Optimization[32] and RPO.[33] Here, the NasNet detects whether it is normal or abnormal. The normal is symbolized as ϖ_1, and the abnormal as ϖ_2.

Architecture of NasNet

The feature H is forwarded to the NasNet technique, which is a neural search architecture that encompasses convolutional cells. The normal cell as well as reduction cell are the two functions of the NasNet approach. The normal cells return the feature map with similar input dimensionality. Likewise, the reduction returns the height as well as the width of the feature mapping. Finally, normal cells, the global_average pooling, flatten layer, and global_max pooling were subjected. The tensor dimensionality is reduced in the last two layers. Arithmetic averages are obtained in the global_average pooling and increased numbers are obtained in the global_max pooling layer during the utilization of the filter. The extracted features are fed into NasNet, a deep neural architecture known for its adaptability in image classification. NasNet learns hierarchical patterns to distinguish between normal and abnormal cases. Flattened layer output is combined in the concatenate layer to evade the network overfitting issue and in the end, it is fed to the dense layer. Further, the SoftMax function of NasNet is demarcated as,

$$d^n = \beta(q_1^n) \quad \ldots (10)$$

$$\beta(q_1^n) = \frac{exp^{q_1^n}}{\sum_{x=1}^{X} exp^{q_1^n}} \quad \ldots (11)$$

where, the probability distribution is termed as $\sum q_1$. Assume, D and Q characterize two metric spaces, as well as $k_1: D \to Q$ is the target function which is established only on fixed aggregate points $k_1(D^1), \ldots, k_1(D^8)$, and the label of objects $D^1, \ldots, D^8$ are known. The object D is fragmented to classes cancer detection denoted as L_N, as given by,

$$L_N\{o \in D | k_1(o) = N\} atN \in \{1, \ldots, 8\}: D = \bigcup_{L}^{N=1} L_N \quad \ldots (12)$$

The target operation $k_1: D \to Q$ that discriminates well across several class labels, is signified as the neural network functioning approach as expressed beneath

$$F_1 = \beta(\sum_{\alpha=1} \mu_{1X}^n H_X^{n-1} + l_x^n) \quad \ldots (13)$$

Here, H denotes the activation component of the vector, whereas the weight of the individual layer n is referred to as μ^n with row x, and X respectively, and the bias is emphasized as l. Equation (13) in compact vectorized form is shown as below,

$$F_2 = \sum_{c_1} \mu^n H^{n-1} + l^n \quad \ldots (14)$$

The outcome of the NasNet model is indicated as F_2. The output of NasNet provides the initial decision on whether a CT scan indicates lung cancer. The pictorial representation of the NasNet is portrayed in Fig. 2.

Testing of NasNet using ARPO

The ARPO applied for fine-tuning the NasNet is obtained by associating the Adam Optimization and RPO. Adam optimization is a widely known algorithm for optimization in DL. Adam is effectually adaptive to learning rates for various parameters and it guarantees rapid convergence and better generalization in DL models. RPO imitates the normal behavior of red pandas, such as foraging and

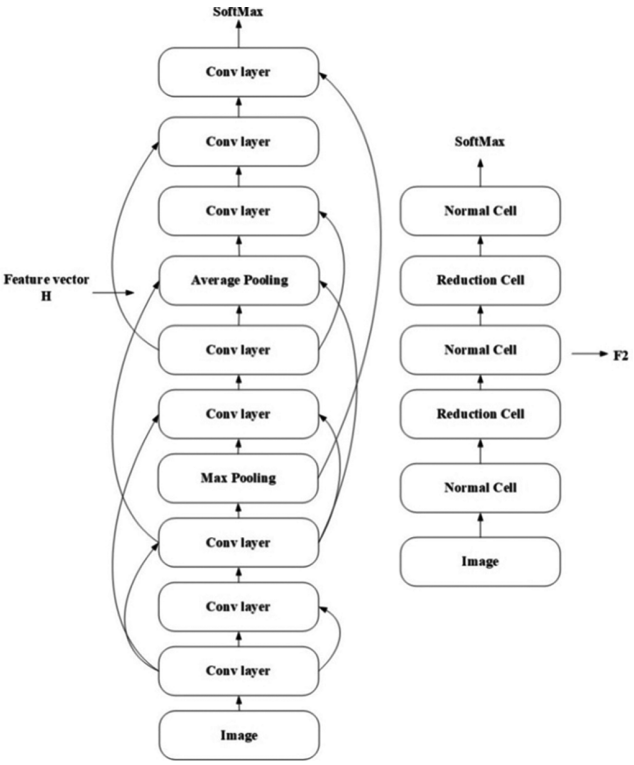

Fig. 2 — Outline of the NasNet approach

climbing trees. RPO is effectual in resolving optimization complexities, its effectiveness is superior when compared with other algorithms, and it has great potential in exploration as well as global search. Hence, the unification of Adam Optimization and RPO provides improved efficiency. The following segment elucidates the steps of the introduced ARPO.

Step 1. Initialization

The RPO technique is a metaheuristic process concerning the red panda population, which is a member of this algorithm. Individual red Panda is referred to as the solution of the candidate to the issue, that recommends specific values to complex variables with respect to its search space location. The initialization of the location of the red panda in the search space is accomplished subsequently, to optimize NasNet training, we introduce Adam Red Panda Optimization (ARPO), a hybrid technique combining Adam's fast adaptive learning with RPO's strong global search capability. This improves both convergence speed and classification robustness,

$$C = \begin{bmatrix} C_1 \\ C_a \\ C_\phi \end{bmatrix}_{\phi \times \nu} = \begin{bmatrix} B_{1,1} B_{1,\tau} B_{1,\nu} \\ B_{a,1} B_{a,\tau} B_{a,\nu} \\ B_{\phi,1} B_{\phi,\tau} B_{\phi,\nu} \end{bmatrix} \quad \ldots (15)$$

$$B_{a,\tau} = \eta r_\tau + t'_{a,\tau}.(wr_\tau - \eta r_\tau), a = 1,..,\phi b = 1,\ldots,\nu \quad \ldots (16)$$

where, C_a designates the a^{th} red panda, $B_{a,\tau}$ signifies its τ^{th} dimension, the number of complex variables is termed as ν, location of the red panda in the population matrix is embodied as C, the population size of red pandas is implied as ϕ, wr_τ and ηr_τ are the lower and upper limits of τ^{th}complex variable and the random number is indicated as $t'_{a,\tau}$which lie between$[0,1]$.

Step 2: Fitness Function

The finest output has a minimum error evaluated concerning Mean Square Error (MSE) and the fitness is expressed as

$$MSE = \frac{1}{\sigma}\sum_{\omega=1}^{\sigma}(F_2^* - F_2)^2 \quad \ldots (17)$$

where, the NasNet outcome is referred to as F_2, the sum of the testing sample is denoted a σ, and the expected result is indicated as F_2^*.

Step 3: Phase 1-Foraging (Exploration)

In this step, the red panda position is labelled according to their movement in search of food. Red pandas are highly capable of finding as well as travelling to forage with their high potential in hearing, vision, as well as smelling. The set of presented locations of food resources for individual pandas concerning the correlation of values of the objective function is expressed as

$$PFS_a = \{C_\rho | \rho \in \{1,2,\ldots,\phi\} and\ E_\rho < E_a\} \cup \{C_{best}\} \quad \ldots (18)$$

Here, E embodies the objective function computed using Eq. (17), C_{best} implies the red panda position with the finest objective operation value, and PFS_a symbolizes the set of established sources of food for a^{th} red pandas. For modeling the red panda's behavior at the time of food search, a novel location is evaluated for individual red pandas regarding movement towards the foraging location as follows,

$$C_a^{\gamma 1}: B_{a,\tau}^{\gamma 1} = B_{a,\tau} + t'(SFS_{a,\tau} - W.B_{a,\tau}) \quad \ldots (19)$$

where, Wstands fora number chosen randomly in the range $\{1,2\}$, t' signifies the random number among the range $[0,1]$, $C_a^{\gamma 1}$ elucidates the updated place of the a^{th} red panda in the initial RPO phase, SFS_a indicates the designated food source for a^{th} the red panda, $C_{a,\tau}^{\gamma 1}$ is its τ^{th} dimension, and $SFS_{a,\tau}$implies its τ^{th} dimension. The above-mentioned equation may be expressed as,

$$B_{a,\tau}(M+1) = B_{a,\tau}(M) + t'\left(SFS_{a,\tau} - W.B_{a,\tau}(M)\right) \quad \ldots (20)$$

$$B_{a,\tau}(M+1) = B_{a,\tau}(M) + t'.SFS_{a,\tau} - t'.W.B_{a,\tau}(M) \quad \ldots (21)$$

$$B_{a,\tau}(M+1) = B_{a,\tau}(M)\left[1 - t'.W\right] + t'.SFS_{a,\tau} \quad \ldots (22)$$

By incorporating Adam optimization into RPO, the convergence can be improved, the. From Adam,

$$B_{a,\tau}(M) = B_{a,\tau}(M-1) - \psi.\hat{\nu}(M)/\sqrt{\hat{K}(a) + \varepsilon} \quad \ldots (23)$$

Substituting Eq. (23) in (22) we get,

$$B_{a,\tau}(M+1) = \left(B_{a,\tau}(M-1) - \psi.\hat{\nu}(M)/\sqrt{\hat{K}(a) + \varepsilon}\right)\left(1 - t'.W\right) + t'.SFS_{a,\tau} \quad \ldots (24)$$

Here, ψ emphasize the constant parameter, bias-corrected first moment estimate is signified as $\hat{\nu}(M)$, $\hat{K}(a)$ designates the bias-corrected second raw

moment estimate, and ε is a constant with value of 10^{-8}. By merging Adam and RPO, ARPO ensures more stable and accurate optimization than traditional single optimizers

Step 4: Phase 2-Climbing and Resting on the Tree (Exploitation)

In this step, the modeling of the location of the red panda is done with respect to the climbing skills of pandas on trees as well as resting there. To label the normal activities of red pandas while climbing on trees, initially, novel location is examined for individual red pandas by employing

$$B_{a,\tau}^{\gamma 2} = B_{a,\tau} + \frac{\eta r_{\tau}.(wr_{\tau} - \eta r_{\tau})}{M}, a = 1,..,\phi b = 1,....,\nu M = 1,2,...,m^{'} \quad \ldots (25)$$

where, $t^{'}$ represents the random number in the range[0,1], $B_{a,\tau}^{\gamma 2}$ is the novel position of the a^{th} red panda in the τ^{th} dimension, the maximal count of iteration is signified as $m^{'}$, and M characterizes the iteration counter.

Step 5: Feasibility Assessment

The updated fitness solution is assessed, and the least fitness solution is selected as the ideal solution.

Step 6: Termination

Till the maximal iteration is attained, the procedure is continued to acquire the finest solution. Thus, the ARPO_NasNet effectively identifies lung cancer from the CT images. In case, the detected output indicates the presence of cancer, the result attained F_2 is subjected to lung cancer severity classification.

Severity Level Classification

The abnormal resultF_2 detected is subjectedto the severity level classification module. Here, the detected outcome is categorized as abnormal, and normalalso, the severity level is categorized as severe, moderate, and mild by utilizingNasNet with ARPO. The operation of the NasNet is mentioned in section 3.5.1 and the steps of the ARPO are labelled in section 3.5.2.

Evaluation Metrics

The proposed ARPO_NasNet model for classifying severity level and identifying lung cancer using CT image, evaluated with various measures with Python Tool is elucidated in this segment. The LIDC-IDRI dataset[34] encompasses the prognostic, as well as the screening of lung cancer using thoracic CT, scans with increased annotated lesions. It is accessed through the web and is an international resource for tuning, progress and estimation of CAD approaches for the prognosis and detection of lung cancer. This dataset contains 1018 cases. The ARPO_NasNet is analyzed based on measures comprising recall, F1-score, accuracy, and precision.

a) Accuracy: The entirety of accurate detections from the overall detection is demarcated as accuracy and is expressed as,

$$\omega_1 = \frac{G_{TP}+G_{TN}}{G_{TP}+U_{FP}+G_{TN}+U_{FN}} \quad \ldots (26)$$

where, the False Positive is embodied as U_{FP}, the False Negative is signified as U_{FN}, the True Positive is emphasized as G_{TP}, the True Negative is implied as G_{TN}, and ω_1 explicates the accuracy. Finally, the model's performance is evaluated using standard classification metrics—accuracy, recall, precision, and F1-score—which provide a comprehensive understanding of detection quality.

b) Recall: The percentage of accurate true positive detection to the entire positive samples applied to ARPO_NasNet is defined as recall and is formulated as,

$$\omega_2 = \frac{G_{TP}}{G_{TP}+U_{FN}} \quad \ldots (27)$$

where, the recall is symbolized as ω_2.

c) Precision: Precision is utilized to find the efficacy of the ARPO_NasNet in true positive detection and is designated as

$$\omega_3 = \frac{G_{TP}}{G_{TP}+U_{FP}} \quad \ldots (28)$$

Here, the precision is termed as ω_3.

d) F1-score: The harmonic means between the recall as well as precision of the ARPO_NasNet is demarcated as F1-score and is represented as

$$\omega_4 = 2 * \frac{\omega_2 * \omega_3}{\omega_2 + \omega_3} \quad \ldots (29)$$

where, the F1-score is indicated as ω_4.

Results and Discussion

Visual Samples

The process of ARPO-NasNet lung cancer detection is illustrated in Fig. 3 in steps. Image (a) denotes the input image of the CT scan that is further used to eliminate noise (b). The segmented lung lobes in Image (c) were obtained after the application of DFC, which is essential to target the pertinent lung parts. Lastly, image (d) represents the LGP features,

extracted out of the segmented image, and utilized in the classification. This animation shows that ARPO_NasNet is an efficient method to prepare and analyze CT images to detect cancer accurately.

Comparative Assessments

The established ARPO_NasNet approach is compared with different recent similar methods to analyze its efficacy. The approaches selected for correlation are DenseNet-121+MobileNet V3[5], PSSO-based DRN[3], MixNet-LD[16] and EOSA-CNN.[17] The efficacy of the ARPO_NasNet is related to different methods concerning the training set and is explained beneath. ARPO_NasNet's performance against several recent methods regarding the training set have been compared and illustrated through Fig. 4. With a training set of 90%, the F1-score recorded by introduced ARPO_NasNet is 92.022%. The accuracy, recall, precision, and F1-score of ARPO_NasNet have observed improvement than those of DenseNet-121+MobileNet V3 and other methods. This demonstrates that ARPO_NasNet, with its hybrid optimization approach, provides superior performance across all metrics. Specifically, the recall of 93.166% suggests that ARPO_NasNet is highly efficient at identifying true positives, which is crucial for cancer detection where false negatives must be minimized. In comparison, DenseNet-121+MobileNet V3 only achieved 85% recall, highlighting the added value of ARPO optimization in our model.

Performance Estimation and Comparative Discussion

The performance evaluation of ARPO_NasNet using the training set across several metrics is illustrated in Fig. 5. The comparative analytical demonstration of the established ARPO_NasNet is demonstrated in Table 2. The designed ARPO_NasNet attained the maximal accuracy, recall, precision, and F1-score of 91.658%, 93.166%, 92.346%, and 92.022% while concerning the training set of 90%. Further, the implementation of the ARPO for testing the NasNet improved the detection and severity level classification for lung cancer. The performance of ARPO_NasNet was evaluated using the training set with varying population sizes (Table 3).

Comprehensive performance metrics of ARPO_NasNet have been depicted through Fig. 5, demonstrating its robustness across accuracy, recall,

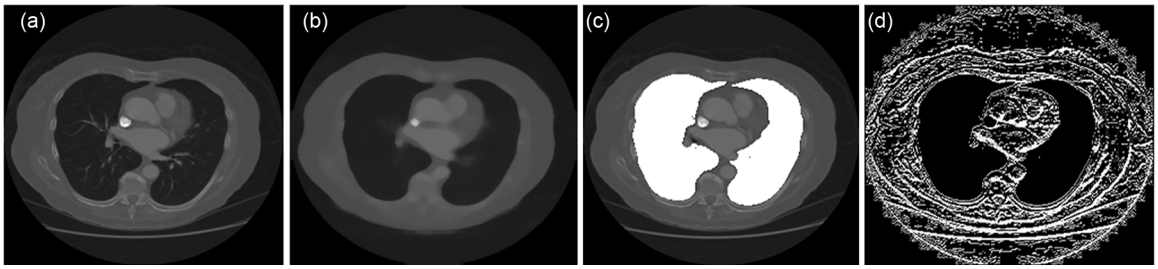

Fig. 3 — Image result of ARPO_NasNet: (a) input image, (b) pre-processing, (c) lung lobe segmented, and (d) LGP feature images

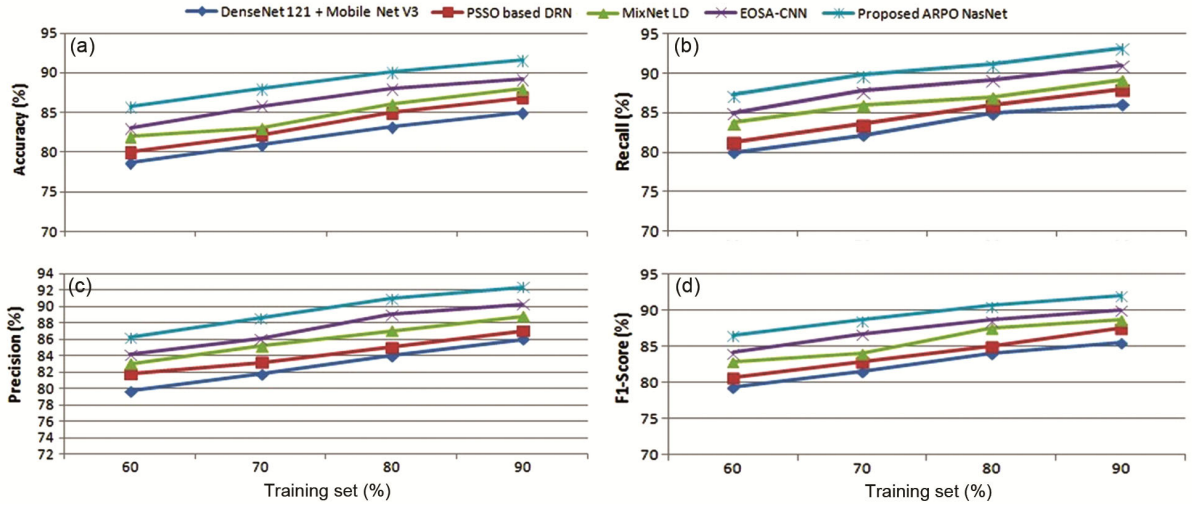

Fig. 4 — Comparative assessment of ARPO_NasNet with training set using: (a) accuracy, (b) Recall, (c) Precision, (d) F1-score

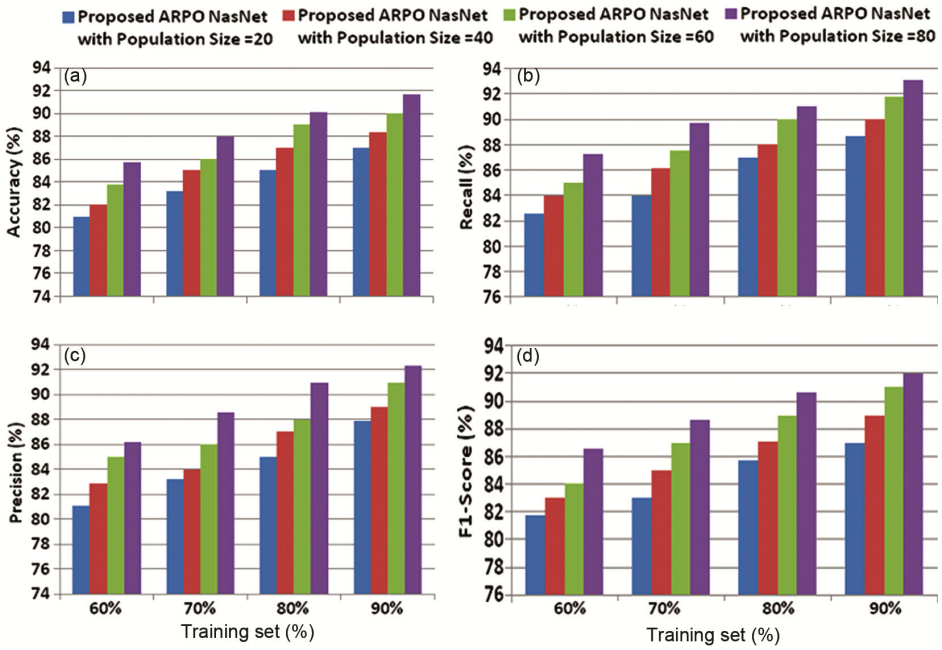

Fig. 5 — The Investigation of ARPO_NasNet with training set using: (a) accuracy, (b) Recall, (c) Precision, and (d) F1-score

Table 2 — Comparative analysis with state-of-the-art algorithms

S.No.	Metrics	Training set	Batch-size	LR	[5]DenseNet 121 + Mobile Net V3	[3]PSSO based DRN	[16]MixNet LD	[17]EOSA-CNN	Proposed ARPO NasNet
1	Accuracy (%)	60%	32	0.001	78.766	80.000	81.997	83.006	85.767
2		70%	32	0.0001	80.998	82.177	83.088	85.768	87.997
3		80%	32	0.00001	83.168	84.997	86.008	88.000	90.153
4		90%	32	0.000001	85.000	86.875	88.001	89.156	91.658
1	F1-Score (%)	60%	32	0.001	79.296	80.674	82.918	84.206	86.515
2		70%	32	0.0001	81.582	82.861	84.042	86.757	88.600
3		80%	32	0.00001	84.083	85.023	87.578	88.589	90.620
4		90%	32	0.000001	85.437	87.436	88.589	90.067	92.022
1	Precision (%)	60%	32	0.001	79.677	81.779	83.009	84.156	86.163
2		70%	32	0.0001	81.768	83.176	85.176	86.008	88.576
3		80%	32	0.00001	84.008	85.009	86.999	88.976	90.977
4		90%	32	0.000001	85.998	87.008	88.768	90.279	92.346
1	Recall (%)	60%	32	0.001	80.000	81.348	83.787	85.007	87.264
2		70%	32	0.0001	82.166	83.546	85.998	87.746	89.775
3		80%	32	0.00001	84.998	86.008	87.008	89.178	91.086
4		90%	32	0.000001	86.008	87.998	89.176	91.000	93.166

Table 3 — Comparative analysis with different population size for proposed model

S.No.	Metric	Training-Set: Testing Set	LR	Proposed ARPO NasNet with Population Size =			
				20	40	60	80
1	F1-Score % Accuracy %	60%: 40%	0.001	80.989	82.001	83.766	85.766
2		70%: 30%	0.0001	83.168	84.998	86.008	87.997
3		80%: 20%	0.00001	85.008	86.998	88.995	90.153
4		90%: 10%	0.000001	87.000	88.347	90.007	**91.658**
1		60%: 40%	0.001	81.787	83.001	84.008	86.515
2		70%: 30%	0.0001	83.009	84.998	86.997	88.600
3		80%: 20%	0.00001	85.767	87.078	89.001	90.620
4		90%: 10%	0.000001	86.997	88.997	90.997	**92.022**

(*Contd.*)

Table 3 — Comparative analysis with different population size for proposed model (*Contd*.)

S.No.	Metric	Training-Set: Testing Set	LR	Proposed ARPO NasNet with Population Size =			
				20	40	60	80
1	Precision %	60%: 40%	0.001	81.078	82.889	84.998	86.163
2		70%: 30%	0.0001	83.168	84.009	85.997	88.576
3		80%: 20%	0.00001	85.009	86.998	88.008	90.977
4		90%: 10%	0.000001	87.890	89.008	90.998	**92.346**
1	Recall %	60%: 40%	0.001	82.567	84.010	85.008	87.264
2		70%: 30%	0.0001	84.008	86.167	87.566	89.775
3		80%: 20%	0.00001	87.000	88.001	89.998	91.086
4		90%: 10%	0.000001	88.654	90.008	91.768	**93.166**

precision, and F1-score. Specifically, ARPO_NasNet achieved 91.658% accuracy and 93.166% recall, which surpasses the performance of MixNet-LD[16] and EOSA-CNN[17] by approximately 4.16% and 2.38% respectively. The improvements in these metrics are likely attributed to the combination of Adam and Red Panda Optimization (ARPO), which helps in overcoming optimization challenges commonly seen in traditional methods.

Conclusions

In this study, a deep learning–based novel hybrid framework, ARPO_NasNet, was proposed for the detection of lung cancer and the assessment of its severity level. The model classifies lung conditions into normal and abnormal categories and further determines the severity as mild, moderate, or severe. The experimental results demonstrate that the proposed ARPO_NasNet model achieves promising performance with an accuracy of 91.658%, recall of 93.166%, precision of 92.346%, and F1-score of 92.022%. These results indicate that the proposed approach can effectively assist in the early detection and severity evaluation of lung cancer, which may support healthcare professionals in diagnosis and treatment planning. However, the current study has certain limitations, as the model was evaluated using only a single dataset, which may affect the generalizability of the results. Future work will focus on validating the model using multiple datasets and larger clinical data, which may further improve its robustness and applicability in real-world medical diagnosis.

Funding Statement

This project does not involve any funding.

Declaration of Competing Interest

None.

Data Set Availability Statement

The Image Database Resource Initiative (IDRI) and The Lung Image Database Consortium (LIDC) has been taken from "https://www.cancerimagingarchive.net/collection/lidc-idri/" accessed on April 2024.

References

1 Tiwari A, Hannan S A, Pinnamaneni R, Al-Ansari A R M, El-Ebiary Y A B, Prema S, Manikandan R & Vidalón J L J, Optimized ensemble of hybrid RNN-GAN models for accurate and automated lung tumour detection from CT images, *Int J Adv Comput Sci Appl*, **14(7)** (2023).

2 Thanammal K K, Lung cancer detection via deep learning-based pyramid network with honey badger algorithm, Measurement, *Sensors*, **31** (2024) 100993.

3 Choudhury A, Balasubramaniam S, Kumar A P & Kumar S N P, PSSO: Political squirrel search optimizer-driven deep learning for severity level detection and classification of lung cancer, *Int J Inf Technol Decis Mak*, (2023) 1–34.

4 Thakur S K, Singh D P & Choudhary J, Lung cancer identification: A review on detection and classification, *Cancer Metastasis Rev*, **39(3)** (2020) 989—998.

5 Wahab Sait A R, Lung cancer detection model using deep learning technique, *Appl Sci*, **13(22)** (2023) 12510.

6 Paing M P, Hamamoto K, Tungjitkusolmun S & Pintavirooj C, Automatic detection and staging of lung tumors using locational features and double-staged classifications, *Appl Sci*, **9(11)** (2019) 2329.

7 Ozdemir O, Russell R L & Berlin A A, A 3D probabilistic deep learning system for detection and diagnosis of lung cancer using low-dose CT scans, *IEEE Trans Med Imaging*, **39(5)** (2019) 1419–1429.

8 Manogaran G, Shakeel P M, Hassanein A S, Kumar P M & Babu G C, Machine learning approach-based gamma distribution for brain tumor detection and data sample imbalance analysis, *IEEE Access*, **7(2024)** (2018) 12–19.

9 Singh V & Kaushik V D, DTCWTASODCNN: DTCWT based weighted fusion model for multimodal medical image quality improvement with ASO technique & DCNN, *J Sci Ind Res*, **81** (2022) 850–858.

10 Niu S, Singh V, Kumar A, Verma D K, Kumar S, Kaushik V D, Chen Z & Joshi K, DCNN-HBA: Honey badger optimization and deep convolutional neural network based a novel hybrid model for producing quality image: HBA-DCNN: Honey Badger Optimization and DCNN based Quality Image Model, *J Sci Ind Res*, **82(12)** (2023) 1304–1315.

11 Cui S, Ming S, Lin Y, Chen F, Shen Q, Li H, Chen G, Gong X & Wang H, Development and clinical application of deep learning model for lung nodules screening on CT images, *Sci Rep*, **10(1)** (2020) 13657.

12 Cao Y, Liu L, Chen X, Man Z, Lin Q, Zeng X & Huang X, Segmentation of lung cancer-caused metastatic lesions in bone scan images using self-defined model with deep supervision, *Biomed Signal Process Control*, **79** (2023) 104068.

13 Padmanandam K, Khilar R, Pitla N, Dhanaraj R K, Pamucar D & Balusamy B, Residual partial derivative multilayer perceptron deep learning based classifier for lung cancer detection, (2023), DOI: 10.21203/rs.3.rs-3680326/v1.

14 Gayap H T & Akhloufi M A, Deep machine learning for medical diagnosis, application to lung cancer detection: A review, *Bio Med Informatics*, **1** (2024) 236–284,

15 Naseer I, Akram S, Masood T, Rashid M & Jaffar A, Lung cancer classification using modified U-Net based lobe segmentation and nodule detection, IEEE Access, (2023).

16 Ahoor A, Arif F, Sajid M Z, Qureshi I, Abbas F, Jabbar S & Abbas Q, MixNet-LD: An automated classification system for multiple lung diseases using modified mixnet model, *Diagnostics*, **13(20)** (2023) 3195.

17 Mohamed T I, Oyelade O N & Ezugwu A E, Automatic detection and classification of lung cancer CT scans based on deep learning and ebola optimization search algorithm, Plos one, **18(8)** (2023) e0285796.

18 Sait W, Rahaman A, Lung cancer detection model using deep learning technique, *Appl Sci*, **13(22)** (2023) 2076–3417. DOI: 10.3390/app132212510.

19 Gayap H T & Akhloufi M A, Deep machine learning for medical diagnosis, application to lung cancer detection: A review, *Bio Med Informatics*, **4** (2024) 236–284, DOI: 10.3390/biomedinformatics4010015.

20 Kanan M, Alharbi H, Alotaibi N, Almasuood L, Aljoaid S, Alharbi T, Albraik L, Alothman W, Aljohani H, Alzahrani A & Alqahtani S, AI-driven models for diagnosing and predicting outcomes in lung cancer: A systematic review and meta-analysis, *Cancers*, **16(3)** (2024) 674, DOI: 10.3390/ cancers16030674.

21 Shafi I, Din S, Khan A, Díez I D, Casanova R D, Pifarre K T, Ashraf I, An effective method for lung cancer diagnosis from CT scan using deep learning-based support vector network, *Cancers*, **14(21)** (2022) 5457, DOI: 10.3390/ cancers14215457.

22 Uddin J, Attention-based DenseNet for lung cancer classification using ct scan and histopathological images, *Designs*, **8(2)** (2024) 27, DOI: 10.3390/designs8020027.

23 Thanoon M A, Zulkifley M A, Mohd Zainuri M A & Abdani S R, A review of deep learning techniques for lung cancer screening and diagnosis based on CT images, *Diagnostics*, **13(16)** (2023) 2617, DOI: 10.3390/diagnostics13162617.

24 Mercaldo F, Tibaldi M G, Lombardi L, Brunese L, Santone A, Cesarelli M, An explainable method for lung cancer detection and localisation from tissue images through convolutional neural networks, Electronics, **13(7)** (2024) 2079–9292. DOI: 10.3390/electronics13071393.

25 Alsheikhy A A, Said Y, Shawly T, Alzahrani A K & Lahza H, A CAD system for lung cancer detection using hybrid deep learning techniques, *Diagnostics*, **13(6)** (2023) 1174, DOI: 10.3390/diagnostics13061174.

26 V R Nitha & Chandra S S V, ExtRanFS: An automated lung cancer malignancy detection system using extremely randomized feature selector, *Diagnostics*, **13(13)** (2023) 2206, DOI: 10.3390/diagnostics13132206.

27 Ahmed A A, Fawi M, Brychcy A, Abouzid M, Witt M & Kaczmarek E, Development and validation of a deep learning model for histopathological slide analysis in lung cancer diagnosis, *Cancers*, **16(8)** (2024) 1506, DOI: 10.3390/cancers16081506. Song Y & Liu, J, An improved adaptive weighted median filter algorithm, in *J Phy: Conf Series*, **1187(4)** (2019) 042107.

28 Feng Q, Chen L, Chen C P & Guo L, Deep fuzzy clustering—a representation learning approach, *IEEE Trans Fuzzy Syst*, **28(7)** (2020) 1420–1433.

29 Habiba U, Howlader M R, Faisal R H & Rahman M M, HLGP: A modified local gradient pattern for image classification, in *Proc Int Conf Electrical, Comput & Commun Eng*, (2019) 1–6.

30 Cano E, Mendoza-Avilés J, Areiza M, Guerra N, Mendoza-Valdés J L & Rovetto C A, Multi skin lesions classification using fine-tuning and data-augmentation applying NAS, *Peer J Comput Sci*, **7** (2021) e371.

31 Jeevidha S, Saraswathi S & Margret A A, Hyperparameter tuning in ECG image classification in GAN model using ADAM optimization, *Int J Innov Res Comput Commun Eng*, **11(5)** (2023) 4128–4136.

32 Givi H, Dehghani M & Hubálovský Š, Red panda optimization algorithm: An effective bio-inspired metaheuristic algorithm for solving engineering optimization problems, *IEEE Access*, (2023).

33 The lung image database consortium (LIDC) and image database resource initiative (IDRI) taken from "https://www.cancerimagingarchive.net/collection/lidc-idri/" (Accessed on April 2024).

34 Xiong W, Zhang G, Yan D, Cao L, Huang X & Li D, Multichannel feature fusion network-based technique for heart sound signal classification and recognition, *Expert Syst Appl*, 273 (2025) 126839, DOI: 10.1016/j.eswa.2025.126839.

35 Xiang F, Li Z, Jiang S, Li C, Li S, Gao T & Zhang J, Multimodal masked autoencoder based on adaptive masking for vitiligo stage classification, *J Imaging Inform Med*, (2025) 01521–7, DOI: 10.1007/s10278-025-01521-7.

36 Yin L, Wang L, Lu S, Wang R, Yang Y, Yang B & Zheng W, Convolution-transformer for image feature extraction, *Comput Model Eng Sci*, **141(1)** (2024) 87–106, DOI: 10.32604/cmes.2024.051083.

37 Song W, Wang X, Guo Y, Li S, Xia B & Hao A, CenterFormer: A novel cluster center enhanced transformer for unconstrained dental plaque segmentation, *IEEE Trans Multimedia*, **26** (2024) 10965–10978, DOI: 10.1109/TMM. 2024.3428349

38 Zhang X, Zhang S, Zhang X, Xiong J, Han X, Wu Z & Chen D, Fast virtual stenting for thoracic endovascular aortic repair of aortic dissection using graph deep learning, *IEEE J Biomed Health Inform*, **29(6**) (2025) 4374–4387, DOI: 10.1109/JBHI.2025.3540712.

39 Jiang R, Yin X, Yang P, Cheng L, Hu J, Yang J & Lv H, A transformer-based weakly supervised computational pathology method for clinical-grade diagnosis and molecular marker discovery of gliomas, *Nat Mach Intell*, **6(8)** (2024) 876–891, DOI: 10.1038/s42256-024-00868-w.

40 Song Z & Yang B, Ant colony based fish crowding degree optimization algorithm for magnetic resonance imaging segmentation in sports knee joint injury assessment, *Expert Syst*, **40(4)** (2023) e12849, DOI:DOI: 10.1111/exsy.12849.